






RESEARCH ARTICLE

10.1029/2022SW003346

NOAA Space Weather Prediction Center Radiation Advisories for the International Civil Aviation Organization

H. M. Bain^{1,2} , K. Copeland³ , T. G. Onsager², and R. A. Steenburgh² 

¹Cooperative Institute for Research in Environmental Sciences, University of Colorado Boulder, Boulder, CO, USA, ²Space Weather Prediction Center, NOAA, Boulder, CO, USA, ³Protection and Survival Research Laboratory, U.S. Federal Aviation Administration, Civil Aerospace Medical Institute, Oklahoma City, OK, USA

Key Points:

- Radiation advisories for the International Civil Aviation Organization (ICAO) provide regional information for users
- During GLE69 the ICAO SEVERE radiation threshold was exceeded in the polar and mid latitude bands down to 32,000 ft
- Based on the current format, large geographic regions are likely to receive unnecessary ICAO radiation advisories

Correspondence to:

H. M. Bain,
hazel.bain@noaa.gov

Citation:

Bain, H. M., Copeland, K., Onsager, T. G., & Steenburgh, R. A. (2023). NOAA Space Weather Prediction Center radiation advisories for the International Civil Aviation Organization. *Space Weather*, 21, e2022SW003346. <https://doi.org/10.1029/2022SW003346>

Received 15 NOV 2022

Accepted 16 JUN 2023

Abstract The National Oceanic and Atmospheric Administration's Space Weather Prediction Center (NOAA/SWPC) issues several solar radiation storm products: the long standing proton Warnings and Alerts that are based on particle intensity levels observed by the Geostationary Operational Environmental Satellites; and the more recent International Civil Aviation Organization (ICAO) radiation advisories which specify effective dose rates at aviation flight levels. SWPC ICAO advisories are supported by the U.S. Federal Aviation Administration (FAA) CARI-7A model. In this paper we use CARI-7A modeling results for the Ground Level Enhancement 69 (GLE69) solar radiation storm which occurred on the 20th of January 2005 to demonstrate the ICAO advisory format. For the onset and peak of GLE69, we find that a severe (SEV) radiation advisory would have been issued for altitudes above 32,000 ft, for polar and mid latitude regions of the northern and southern hemisphere. At lower altitudes, down to 25,000 ft, the moderate (MOD) radiation threshold would have been exceeded. In total, 10 ICAO radiation advisories would have been issued over 6.5 hr. From the retrospective modeling of GLE69, and feedback from users, we identify ways in which the ICAO advisories should be improved.

Plain Language Summary The National Oceanic and Atmospheric Administration's Space Weather Prediction Center (NOAA/SWPC) issues products related to solar radiation storms, defined as periods when the number of energetic particles in space are elevated because of enhanced solar activity. Traditionally these products have been based on observations by NOAA's Geostationary Operational Environmental Satellite, indicating the intensity of the storm outside the Earth's atmosphere. New advisories for the International Civil Aviation Organization (ICAO) alert operators when the radiation environment at aviation flight levels is enhanced. At SWPC, ICAO radiation advisories are supported by the U.S. Federal Aviation Administration CARI-7A model. We present CARI-7A modeling results for a solar radiation storm which occurred on the 20th of January 2005. At the peak of the storm, we find that radiation advisories would have been issued down to 25,000 ft, for polar and mid latitude regions of the northern and southern hemisphere. The issued advisories would have been updated periodically to keep forecast users informed as to which flight levels were impacted. In total, SWPC would have been issuing ICAO radiation advisories for 6.5 hr. The results identify several ways in which the ICAO advisory format could be improved to prevent people receiving unnecessary warnings.

1. Introduction

The National Oceanic and Atmospheric Administration's Space Weather Prediction Center (NOAA SWPC) provides space weather forecasts and real-time situational awareness of the near-Earth space environment. Solar radiation storms, consisting of solar energetic particles (SEPs) accelerated in flares and interplanetary shocks driven by coronal mass ejections (CMEs), are one type of phenomena which can impact this environment. SEPs have the capacity to cause space-based electronic hardware to malfunction (Koons et al., 1999) and disrupt long distance high frequency (HF) radio communications in the polar regions. These events can pose a radiation hazard to astronauts, as well as flight crew and passengers (Copeland et al., 2008; Cucinotta, 2015; Cucinotta et al., 2010, 2013; Mertens & Slaba, 2019).

In this paper we focus on the impacts of large SEP events on the aviation industry. We aim to familiarize researchers and users with new radiation advisories issued by SWPC for the International Civil Aviation Organization (ICAO). In particular, we hope to communicate the differences between SWPC's traditional suite of proton forecasts and the new ICAO advisories; illustrate how these new regional products address user requests

© 2023. The Authors.

This is an open access article under the terms of the [Creative Commons Attribution-NonCommercial-NoDerivs License](https://creativecommons.org/licenses/by-nc-nd/4.0/), which permits use and distribution in any medium, provided the original work is properly cited, the use is non-commercial and no modifications or adaptations are made.

for services tailored to the aviation industry; and highlight some areas where the ICAO radiation advisories should be improved. To do this we model a series of SEP events which occurred in January 2005. We generate the corresponding ICAO advisories that would have been issued by SWPC for such events and compare them to the archived proton forecasts that were issued at that time. To model the radiation environment we use the U.S. Federal Aviation Administration (FAA) CARI-7A aviation dose rate model (Copeland, 2017; Copeland et al., 2008) which was transitioned to operations at SWPC in 2019 to support SWPC ICAO radiation advisories.

We compare the information provided in ICAO radiation advisories to SWPC's traditional short-term Warning and Alert products to demonstrate how ICAO advisories could be used to improve the aviation industry's response to solar radiation storms. For example, the aviation industry has traditionally used Alerts for the S3 level on the Solar Radiation Storm (S-)scale (see Section 4 for details) to indicate a significant enhancement to the radiation environment, requiring flights in the polar regions to be rerouted or delayed. As the S3 level is a global index defined by relatively low energy proton intensity levels in geostationary orbit, there is not a direct correlation with the observed radiation environment in the atmosphere as experienced by flight crew and passengers. In this paper we show the modeling results for two S3 radiation storms and demonstrate that an S3 Alert may not imply a significant increase in radiation dose rates at flight altitudes.

From the January 2005 case study events we identify places where the advisory format should be improved in order to make the information actionable. For example, the current ICAO radiation advisories have very coarse latitudinal resolution that is based on geographic (rather than geomagnetic) coordinates, with no specification of the longitudinal extent. This will likely result in users receiving advisories for regions that are not experiencing enhanced radiation levels.

In the fall of 2022, NOAA SWPC hosted a hands-on Testbed Experiment which brought together researchers, forecasters and representatives from the aviation industry (including Flight Operations, Flight Safety, Dispatch, Meteorology, Pilots Union, Air Traffic Management and Communications Groups) to discuss SWPC's products and services for the aviation industry, including the new ICAO radiation advisories. Based on the modeling results presented in this paper, and feedback from users at the Experiment where these results were shown, we conclude that revisions to the ICAO radiation advisories are required. This should be done in coordination with forecast centers and aviation representatives. Furthermore, we highlight the need for atmospheric radiation measurements to be taken during large SEP events to better validate and improve models and to revise the ICAO advisories in light of modeling capabilities and uncertainties.

2. Background

SWPC radiation storm services have traditionally been based on proton intensity levels in geostationary orbit, as observed by particle sensors on NOAA's Geostationary Operational Environmental Satellites (GOES) (Kress et al., 2020; Rodriguez et al., 2014; Sauer, 1989). Corresponding SWPC radiation products are based on the NOAA Solar Radiation Storm Scale (S-scale: <https://www.swpc.noaa.gov/noaa-scales-explanation>) which relates the GOES ≥ 10 MeV integral proton flux to the impacts on satellite systems, HF communications, navigation systems and biological impacts to astronauts, in addition to crew and passengers on aircraft. However, products based on low energy (≥ 10 MeV) proton intensities in geostationary orbit do not directly communicate to users whether there is an enhancement in the atmospheric radiation environment experienced by the aviation industry (Meier & Matthiä, 2014). To significantly enhance the radiation environment at aviation flight levels requires an increase in proton energies of ≥ 500 MeV to several GeV. These events are typically registered as a Ground Level Enhancement (GLE), that is, a sudden increase in the particle intensities recorded by ground based neutron monitors. The recent NOAA SWPC customer requirements survey (Abt Associates, 2019) highlighted the need for improved space weather products and services tailored to the aviation industry. Geographically targeted forecasts and warnings of the radiation environment, available with longer lead times and confidence intervals were highlighted as requests from users. The new ICAO radiation advisories focus on the impacts of higher energy SEP events, the need for regional situational awareness, and for this information to follow standard practices and language which is consistent with that used by aviators for terrestrial weather services. The advisories should provide actionable, impact based, decision support services for the aviation community.

In 2018 ICAO selected NOAA SWPC as one of three (now four) global space weather forecast centers (SWXC) to provide space weather situational awareness tailored to the requirements of civil aviation. In November 2019,

SWPC began disseminating advisories for space weather phenomena expected to impact HF communications and Global Navigation Satellite System (GNSS)-based navigation, and enhance the radiation environment at the altitudes of civil aircraft. These advisories provide operationally relevant information to aviation operators, aircraft flight crew, air navigation service providers, and civil aviation authorities. This situational awareness allows operators to anticipate and plan for degraded performance of communication and navigation systems and to improve safety margins.

3. CARI-7A Model

Two main sources of ionizing radiation contribute to the radiation environment at aviation altitudes: background galactic cosmic radiation (GCR) consisting of highly energetic particles which originate outside the solar system, for example, in explosive supernovae events; and SEP events associated with transient solar eruptive events which can significantly increase the flux of energetic particles entering the Earth's atmosphere for relatively short periods of time (hours to days). The geomagnetic field controls the access of energetic particles to the atmosphere (Störmer, 1956). The depth to which a particle can penetrate the magnetosphere is dictated by its rigidity, R , (momentum per unit charge). Each location in the Earth's magnetic field has a corresponding geomagnetic cutoff rigidity, R_c that is, the minimum rigidity required to reach that location. Particles with rigidity below this threshold are deflected. Equatorial regions associated with closed geomagnetic fields and high values of R_c , are largely protected from incident radiation. However, regions of open magnetic field, such as those occurring at polar and other high geomagnetic latitudes ($\gtrsim 55^\circ$), can provide little to no protection ($R_c \sim 0$ GV). As such, certain regions of the globe, and therefore certain flight routes, are more susceptible to the effects of ionizing radiation than others. As the Earth's magnetic field responds to the solar wind conditions, the mapping of cutoff rigidity changes.

SWPC radiation advisories for ICAO are based on the CARI-7A aviation dose rate model (Copeland, 2017; Copeland et al., 2008) which calculates effective dose rates resulting from ionizing GCR and SEP radiation entering a dynamically changing magnetosphere. The model framework includes methods for simulating the background GCR flux and specifying the real time SEP particle flux from observations; estimating the variable magnetic shielding as the geomagnetic field dynamically changes; and the response of the atmosphere to incident ionizing radiation. From input SEP and GCR spectra, CARI-7A simulates secondary particle showers in the Earth's atmosphere and corresponding effective dose rates. For details, see Appendix A.

In preparation for the new ICAO space weather advisories, the CARI-7A model was transitioned into real-time forecast operations at NOAA SWPC. For SWPC operations, CARI-7A produces global radiation dose rate maps with a 5 min cadence and a spatial resolution of $5^\circ \times 5^\circ$, see Figure 1. These maps are colorcoded according to ICAO moderate and severe effective dose rate threshold levels (see Section 4.2 below) to clearly communicate to forecasters regions where the radiation environment is significantly enhanced above the background.

4. NOAA SWPC Solar Radiation Storm Products

NOAA SWPC has several solar radiation storm forecasts and products. We give a summary of the existing energetic proton products based on GOES particle observations and of the new ICAO radiation advisories which will complement the existing SWPC services.

4.1. Solar Proton Products

The NOAA S-scale is based on the ≥ 10 MeV integral proton flux observed by GOES. An S1 event occurs when the ≥ 10 MeV integral proton flux exceeds 10 particle flux units (1 p.f.u. = 1 particle/(cm² s sr)). The threshold for an S2 event is one order of magnitude higher at 100 p.f.u., the S3 threshold is 1000 p.f.u. and so on through to the maximum S5 storm level. SWPC issues two types of services for solar protons: long term (1–3 days) probabilistic forecasts and short term (minutes to hours) Warning and Alert hazard products.

4.1.1. 3-Day Probabilistic Forecasts

Long-term, probabilistic forecasts indicate the likelihood of the GOES ≥ 10 MeV integral proton flux exceeding 10 p.f.u. that is, the threshold for an S1 storm, for at least three consecutive 5-min readings in the next 3 days. The

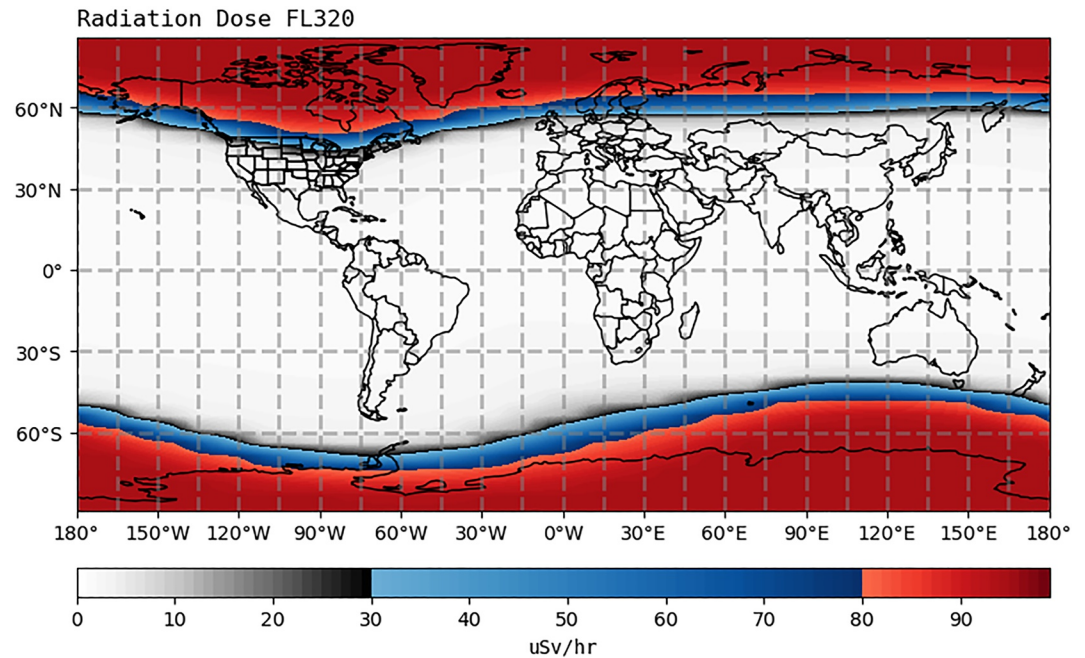


Figure 1. An example of a CARI-7A effective dose rate map at FL320 (32,000 ft) for January 20th at 06:55 UTC. Greyscale indicates effective dose rates below the MOD threshold, blue indicates effective dose rates in the MOD advisory range between 30 $\mu\text{Sv/hr}$ and 80 $\mu\text{Sv/hr}$, and red indicates effective dose rates ≥ 80 $\mu\text{Sv/hr}$ SEV.

3-day proton event probabilities are reported in the SWPC 3-day Forecast product, the Report of Geophysical and Solar Activity (RSGA) (also referred to as the Joint United States Air Force (USAF)/NOAA Solar Geophysical Activity Report and Forecast (SGARF)), and Solar Synoptic Maps. The RSGA/SGARF is issued daily at 22:00 UTC and is valid from 00:00 UTC of the following day while the 3-day Forecast is issued daily at 00:00 UTC and updated at noon. Current products can be found on the SWPC website <https://www.swpc.noaa.gov/products/3-day-forecast>. An archive of historical products is hosted by the NOAA National Centers for Environmental Information (NCEI) and is available at <https://www.ngdc.noaa.gov/stp/spaceweather.html> under Daily Reports. For more details on how these forecasts are prepared and the probabilistic forecast performance metrics and skill over solar cycles 23 and 24, see (Bain et al., 2021). 3-day probabilistic forecasts can be used for planning operations in the coming days, however it is noted that forecast skill decreases significantly going from day 1 to day 2 and 3 forecasts (Bain et al., 2021).

4.1.2. Warning and Alert Products

Warning products are issued when a forecaster believes that an event is imminent or highly likely, providing a short lead time (typically several minutes to several hours), high confidence deterministic forecast. Warnings are issued for the ≥ 10 MeV proton flux exceeding 10 p.f.u. (i.e., the S1 storm threshold) or for the higher energy ≥ 100 MeV proton flux exceeding 1 p.f.u.. An Alert is issued when the proton flux threshold has been exceeded for three consecutive 5-min readings. Alerts are also issued when each of the higher ≥ 10 MeV S-scale threshold levels are exceeded, confirming the onset and progression of the event. Once the event has concluded, a Summary product is issued with details of the event. The Preliminary Report and Forecast of Solar Geophysical Data (PRF of SGD) report issued weekly and produced jointly by NOAA SWPC and the U.S. Air Force Weather Agency (AFWA) contains a record of SWPC Warning and Alert products. An archive of reports issued from 1997 to the present is hosted by NOAA NCEI and is available at <https://www.ngdc.noaa.gov/stp/spaceweather.html>, listed under Periodic Reports and under Weekly Reports. For more details on how the SWPC Warning and Alert products are prepared and the corresponding performance metrics and skill over solar cycles 23 and 24, see (Bain et al., 2021).

4.2. ICAO Radiation Advisory Specifications

The ICAO Global Space Weather Centers follow a mandatory set of requirements as defined by the “Annex 3 to the Convention on International Civil Aviation, Meteorological Service for International Air Navigation, ICAO International Standards and Recommended Practices (SARPs)” (2018) and the “Manual on Space Weather Information in Support of International Air Navigation (Doc 10100)” (2019), as well as an agreed upon set of best practices developed by the ICAO SWXC Coordination Group to maintain advisory consistency across centers.

ICAO advisories are text based and take the form of the example showed in Table 1. As per the international standard, altitudes are communicated in units of feet and issued at 1,000 ft vertical increments between 25,000 ft (i.e., Flight Level 250, abbreviated to FL250) and 60,000 ft (i.e., FL600). The globe is divided into coarse 30° latitude × 15° longitude bins, gray dashed grid in Figure 1. However, radiation advisories are aggregated into six geographic latitude bands only: High Northern Hemisphere (HNH: ≥60°N), Mid Northern Hemisphere (MNH: 30°N – 60°N), Equatorial Northern Hemisphere (ENH: 0° – 30°N), Equatorial Southern Hemisphere (ESH: 0° – 30°S), Mid Southern Hemisphere (MSH: 30°S – 60°S), High Southern Hemisphere (HSH: ≥60°S). Advisories are currently expected to be symmetrical for the northern and southern hemispheres. Two effective dose rate thresholds have been set for ICAO radiation advisories: a moderate (MOD) threshold of 30 μSv/hr, and a severe (SEV) threshold of 80 μSv/hr. As the prime intent of these radiation advisories is to alert airline operators to the occurrence of intense solar radiation storms, issuing alerts for the background GCR is not considered. Due to likelihood that the background GCR could exceed the MOD threshold at the highest flight levels from time to time, MOD advisories will only be issued at FL460 (46,000 ft) and below. Separate advisory products are issued for SEV and MOD threshold crossings, differentiated by the flight levels impacted.

Once an advisory is issued, it will be updated every 6 hours from the nearest hour after the advisory is issued, or sooner if there is a significant change in the environmental conditions. Significant changes include changes to the advisory threshold level or the impacted area, either geographical or vertical, specifically if the impacted flight levels change by at least 6,000 ft (FL60). However, to avoid issuing too many advisories, it is suggested that forecasters wait at least 30 minutes after the previous advisory was issued and/or observe at least three consecutive 5 minute time intervals where the impacted flight levels have changed by 6,000 ft or more before issuing an update. Currently CARI-7A runs as a nowcast. Without accurate predictions of the SEP proton time intensity profile (not yet possible operationally), accurate forecasts are not possible, as such the +6, +12, +18, and +24 hr forecasts are listed as Not Available.

Termination of a MOD or SEV advisory is issued when consecutive dose rate values no longer exceed the ICAO thresholds. It is suggested that the Space Weather Centers wait 45 min after the last threshold was crossed before terminating the advisory: however, SWPC procedures allow for forecaster discretion. For example, should dose rates continue to hover just below a threshold, a forecaster may choose to hold off on issuing a termination to be sure conditions are improving, thus weighing the impact to users if a termination was issued too early and had to be rescinded. For termination advisories, the NXT ADVISORY field reads No Further Advisories.

5. January 2005 Case Study Events

15–22 January 2005 provides an excellent case study for showcasing SWPC solar proton products during a period of intense solar activity and demonstrating the ICAO radiation advisories that would be issued during such a time frame. During this period, solar activity originated largely from NOAA active region 10720 which rotated onto the disk on January 10th as a simple beta magnetic sunspot. Within the next 48 hr the region developed quickly into a large and magnetically complex sunspot group. Between the 14th and end of the 20th, the region produced seventeen M class and four X class flares (see the top row of Figure 2) which were associated with a series of proton events observed at Earth (see the middle row of Figure 2). Table 2 contains details of the X-ray flare class and peak times, and corresponding proton Warning and Alert products that were issued by SWPC during this period, to give an idea of the timescales involved. Note, timings for SWPC proton Summary products issued at the end of a proton event are not listed here.

<p>Table 1 <i>Example ICAO Text Based Radiation Advisory</i></p>	<p>Description</p>
<p>Advisory text</p>	<p>Headers</p>
<p>FNXX03 KWNP 200700</p>	<p>Phenomena (FNXX03 = Radiation) Aerodrome (KWNP = SWPC) Issue Time (day/hour/min)</p>
<p>SWX ADVISORY</p>	<p>Advisory type (SWX = Space Weather)</p>
<p>DTG: 20050120/0700Z</p>	<p>Date and time of advisory</p>
<p>SWXC: SWPC</p>	<p>Issuing space weather center</p>
<p>ADVISORY NR: 2005/1</p>	<p>Advisory record number by year</p>
<p>SWX EFFECT: RADIATION SEV</p>	<p>Space weather phenomena and threshold level</p>
<p>OBS SWX: 20/0700Z HNH MNH MSH HSH E180 - W180 ABV FL330</p>	<p>Information about observed SWX event: time in UTC using format DD/HH/mmZ, latitude bands, longitudinal extent, at or above Flight Level</p>
<p>FCST SWX +6 HR: 20/1300Z NOT AVBL</p>	<p>Forecast 6, 12, 18, and 24 hr from current advisory</p>
<p>FCST SWX +12 HR: 20/1900Z NOT AVBL</p>	
<p>FCST SWX +18 HR: 20/0100Z NOT AVBL</p>	
<p>FCST SWX +24 HR: 20/0700Z NOT AVBL</p>	
<p>RMK:</p>	<p>Forecaster remarks relevant for aviation</p>
<p>NXT ADVISORY: 20050120/1300Z =</p>	<p>Next advisory date/time or "No Further Advisories"</p>

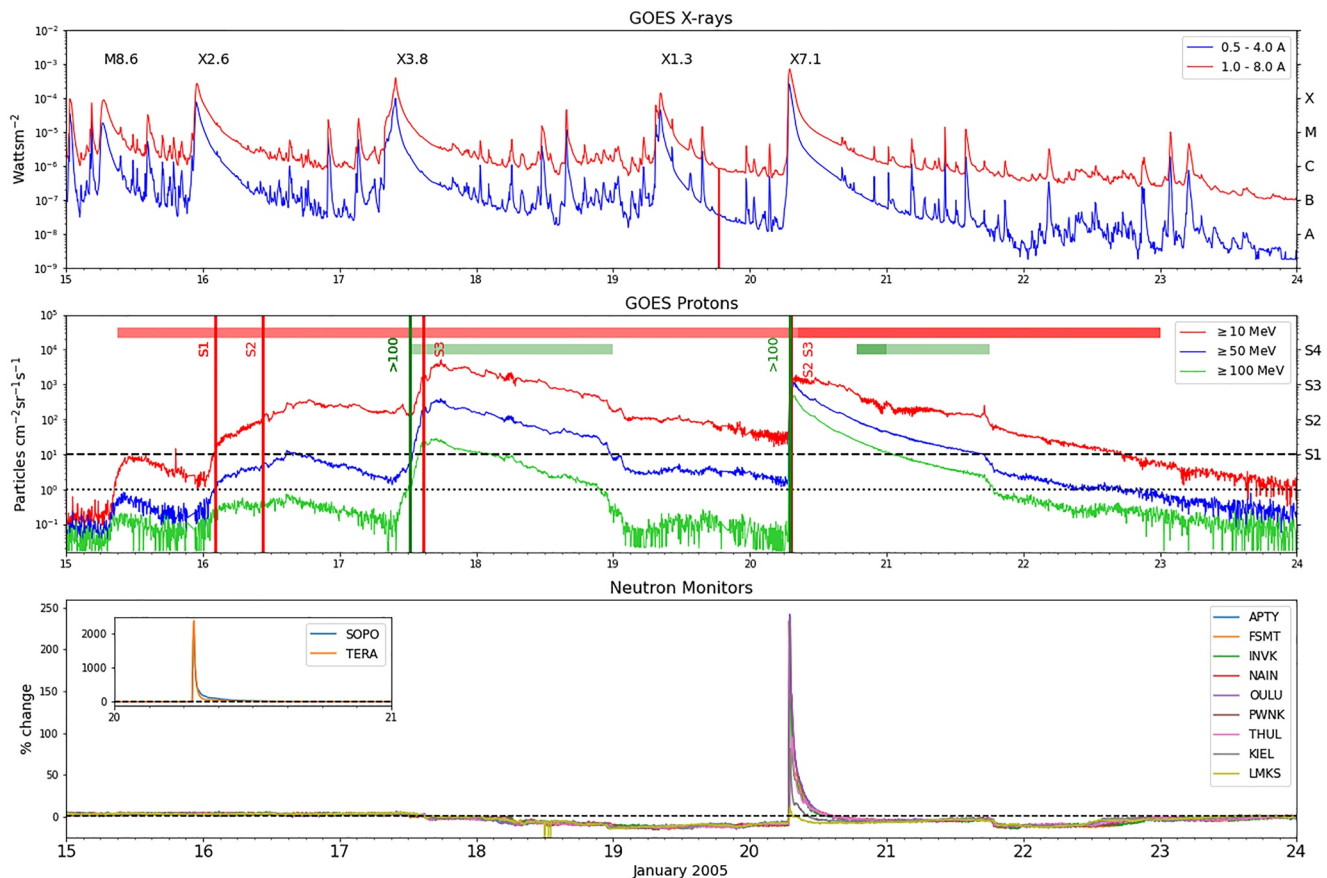


Figure 2. Summary of the January 2005 solar activity. Top: Geostationary Operational Environmental Satellites (GOES) X-rays showing solar flare activity. Middle: GOES ≥ 10 MeV (red), ≥ 50 MeV (blue) and ≥ 100 MeV (green) proton measurements with timings for SWPC ≥ 10 MeV and ≥ 100 MeV Warning (horizontal bars) and Alert (vertical lines) products plotted. Dashed and dotted black lines indicate the ≥ 10 MeV particle flux exceeding 10 p.f.u. (S1 storm) and ≥ 100 MeV particle flux exceeding 1 p.f.u. thresholds. Bottom: Relative change in neutron count rate at selected high latitude neutron monitor stations with inset showing South Pole (SOPO) and Terre Adelie (TERA).

5.1. Initial S1 and S2 Activity

On January 15th, AR10720 was located in the center of the disk. Following an M8.6 flare with an associated fast halo CME, an increase in the ≥ 10 MeV proton flux was observed at GOES. In response to the rising proton flux, SWPC issued an S1 Warning (the horizontal red bar in the middle panel of Figure 2). However the increase did not exceed the 10 p.f.u. S1 threshold (black horizontal dashed line in Figure 2) and subsequently no S1 Alert was issued. Later on the 15th, an X2.6 flare resulted in a larger proton event which crossed the S1 and S2 thresholds. Corresponding S1 and S2 proton Alerts were issued by SWPC, see the vertical red lines in the middle panel of Figure 2, and the S1 proton Warning was extended. As seen in the middle panel of Figure 2, neither of these particle enhancements had a significantly high flux of ≥ 100 MeV protons and consequently were not energetic enough to produce an increase above the background of the neutron count rate observed by the ground-based neutron monitors (bottom panel of Figure 2, see Table 3 for neutron monitor station information). This implies that the radiation environment at aviation altitudes was not significantly altered and as such no ICAO radiation advisory would have been required. The takeaway here is that not all proton events are intense enough to reach the ICAO advisory thresholds. Furthermore, due to continuing solar activity, SWPC S1 proton Warnings can be repeatedly extended to cover multiple days. This may provide useful situational awareness for the aviation industry but may not provide actionable information for flight planning due to the long time frames involved and the indirect relationship between and S1 Warning and a significant radiation enhancement in the atmosphere.

Table 2

X-Ray Flare Class and Peak Timing and Associated NOAA SWPC Warning and Alert Products Issued From the 15th to 22nd of January 2005

Flare class	Flare peak (UTC)	Product	Energy (MeV)	Issue time (UTC)	Valid/Event time (UTC)
M8.6	15 January 06:38	Warning (S1)	≥ 10	15 January 08:55	15 January 09:00–15 January 23:59
X2.6	15 January 23:02	Warning (S1 EXT)	≥ 10	15 January 23:47	15 January 09:00–16 January 23:59
		Alert (S1)	≥ 10	16 January 02:29	16 January 02:10
		Alert (S2)	≥ 10	16 January 10:30	16 January 10:30
		Warning (S1 EXT)	≥ 10	16 January 23:55	15 January 09:00–17 January 23:59
X3.8	17 January 09:52	Warning (≥ 100 MeV)	≥ 100	17 January 12:21	17 January 12:22–17 January 15:00
		Alert (≥ 100 MeV)	≥ 100	17 January 12:40	17 January 12:15
		Alert (S3)	≥ 10	17 January 14:36	17 January 14:10
		Warning (≥ 100 MeV EXT)	≥ 100	17 January 22:22	17 January 12:22–18 January 23:59
		Warning (S1 EXT)	≥ 10	17 January 22:28	15 January 09:00–18 January 23:59
		Warning (S1 EXT)	≥ 10	18 January 22:09	15 January 09:00 - 19 January 23:59
X1.3	19 January 08:21	Warning (S1 EXT)	≥ 10	19 January 23:00	15 January 09:00–20 January 23:59
X7.1	20 January 07:01	Alert (S2)	≥ 10	20 January 07:02	20 January 07:01
		Alert (≥ 100 MeV)	≥ 100	20 January 07:04	20 January 07:01
		Alert (S3)	≥ 10	20 January 07:12	20 January 07:05
		Warning (S1)	≥ 10	20 January 08:30	20 January 08:30 - 20 January 23:59
		Warning (≥ 100 MeV)	≥ 100	20 January 18:45	20 January 18:45–20 January 23:59
		Warning (≥ 100 MeV EXT)	≥ 100	21 January 06:49	20 January 18:45–21 January 18:00
		Warning (S1 EXT)	≥ 10	21 January 06:54	20 January 08:30–21 January 23:59
Warning (S1 EXT)	≥ 10	21 January 23:54	20 January 08:30–22 January 23:59		

5.2. An S3 Event Without an ICAO Radiation Advisory

On the 17th of January an X3.8 flare associated with a fast halo CME produced another proton event. This new event showed a particle increase at higher energies with the ≥ 100 MeV protons crossing the 1 p.f.u. threshold. The ≥ 10 MeV protons, which remained elevated above the S2 threshold since the previous event, showed a further increase and crossed the S3 threshold. In response to this activity SWPC issued a Warning for ≥ 100 MeV exceeding 1 p.f.u.. The S1 Warning was repeatedly extended in response to the continuing solar activity, and corresponding Alerts were issued for each S-scale threshold crossing, see Table 2. Despite another X class flare (X1.3) on the 19th of January, no significant increase was seen to the already elevated proton fluxes.

As with the previous few days, no increase above the background was seen for the ground based neutron monitor stations, again indicating that there was no significant enhancement in the radiation environment at aviation altitudes. However, it is worth noting that the S3 Alert for ≥ 10 MeV protons has historically been used by the aviation community as an indicator of increased radiation and a signal to avoid polar flight routes. At the S3 level it is expected that HF radio communications may be degraded or interrupted as a result of polar cap absorption (PCA) from high energy protons ionizing the D-region of the polar ionosphere. PCA events can last for several days in

Table 3
Neutron Monitor Station Information

Station	ID	Country	Location	Cutoff rigidity (MV)
Terre Adelie	TERA	Antarctica	66.67°S 140.00°E	0
South Pole	SOPO	Antarctica	90.00°S 00.00°E	100
Thule	THUL	Greenland	76.50°N 68.80°E	100
Inuvik	INVK	Canada	68.35°N 133.72°W	180
Fort Smith	FSMT	Canada	60.02°N 111.93°W	300
Nain	NAIN	Canada	56.55°N 61.68°W	300
Apatity	APTY	Russia	67.57°N 33.40°E	650
Oulu	OULU	Finland	65.02°N 25.50°W	810
Kiel	KIEL	Germany	54.30°N 10.10°E	2290
Lomnický štít	LMKS	Slovakia	49.20°N 20.22°E	3840

accordance with the extended presence of lower energy ≥ 10 MeV protons. This can pose a concern for airlines operating at high latitudes above 82° where equatorial geosynchronous satellite communications are not available as an alternative. However, an S3 Alert alone is not sufficient to determine the presence of high energy (≥ 500 MeV) protons and any radiation hazard for flight crew and passengers. While ≥ 100 MeV protons are observed above the 1 p.f.u. threshold during the 17th and 19th of January, the proton spectrum is still not sufficiently energetic to register as a GLE.

5.3. An S3 Event With an ICAO Radiation Advisory

On January 20th, AR10720 produced a large X7.1 solar flare associated with a CME off the northwest limb. A prompt onset SEP was observed by GOES with protons in the ≥ 100 MeV range elevated well above background. The ≥ 10 MeV proton channel, which was still above the S1 threshold at the onset of the event, rose rapidly crossing both the S2 and S3 thresholds and triggered SWPC Alerts. The SWPC ≥ 10 MeV Warning product was further extended to cover the period through January 22nd. It should be noted that

the ≥ 10 MeV peak flux was lower for this event than for the ≥ 10 MeV peak on the 17th, Figure 2. The converse is true for the higher energy ≥ 50 MeV and ≥ 100 MeV particle intensities. This is indicative of the harder, flatter incident proton energy spectrum required to produce a GLE and enhance the atmospheric radiation environment. This event resulted in GLE69, the largest GLE of the solar cycle. The GLE is observed by a number of geographically dispersed neutron monitor stations as a sudden increase in neutron counts above the background level, see the bottom panel of Figure 2.

CARI-7A was used to retrospectively model the radiation environment at ICAO flight levels during this event. Figure 3 shows CARI-7A radiation summary maps produced at SWPC to aid forecasters in visualizing and formulating ICAO advisories. To create a summary map, CARI-7A radiation dose rate maps, such as the one shown in Figure 1, are thresholded to indicate which regions, on the coarse ICAO $30^\circ \times 15^\circ$ grid, exceed MOD and SEV thresholds. Two separate summary maps are produced: one map for SEV advisories and another for MOD advisories. Vertical information is represented in the 2D summary map with color coding to indicate the minimum FL at which the threshold is exceeded. Red and blue/gray color gradients show how deep into the atmosphere the radiation is enhanced above SEV and MOD thresholds, as a function of geographic region. The darker the color the lower in altitude the threshold is crossed. Black vertical colorbars indicate the global flight level minimum, that is, the lowest flight level to exceed a SEV or MOD threshold in any region on the globe. It is this global minimum that is reported in the issued advisory.

5.3.1. Spatial Extent of GLE69 Radiation Impacts

Figure 3 shows thresholded summary maps at the onset of GLE69 at 06:55 UTC, the same time interval as shown in Figure 1. As expected the most impacted regions are located at the northern and southern geomagnetic poles. Over North America, the SEV threshold is exceeded for altitudes as low as FL320 and MOD all the way down to FL250. Meanwhile the airspace over Europe is less impacted. Here, for example, the UK is included in a region labeled as having exceeded the SEV threshold down to FL480 and MOD down to FL340. However it should be noted that the coarse $30^\circ \times 15^\circ$ grid exaggerates the spatial impact of GLE69. From Figure 1 we can see that CARI-7A indicates only the airspace over Canada and Greenland in North America exceeds the SEV threshold, and only the northern states of the U.S. exceeding MOD. However due to the coarse latitude band, the whole U.S. and northern parts of Mexico would be included in SEV and MOD advisories. A similar situation occurs for the UK, and in the southern hemisphere, for Australia and New Zealand. Furthermore, as noted in Section 4.2, advisories are issued for entire latitude bands only. This means, for example, if any portion of a region in the MNH band exceeds the SEV threshold, the entire MNH latitude band is identified in the issued advisory. As advisories are mirrored in the northern and southern hemispheres the entire MSH latitude band will also be included in the advisory. Between the coarse latitude band designation and mirroring of the advisory in both hemispheres, this results in parts of South America and Africa being included in the advisories unnecessarily. The current requirement for radiation advisories to be issued for entire geographic latitude bands will result in users receiving advisories for regions that do not exceed a threshold. Forecaster discretion is likely to play a role for advisories covering

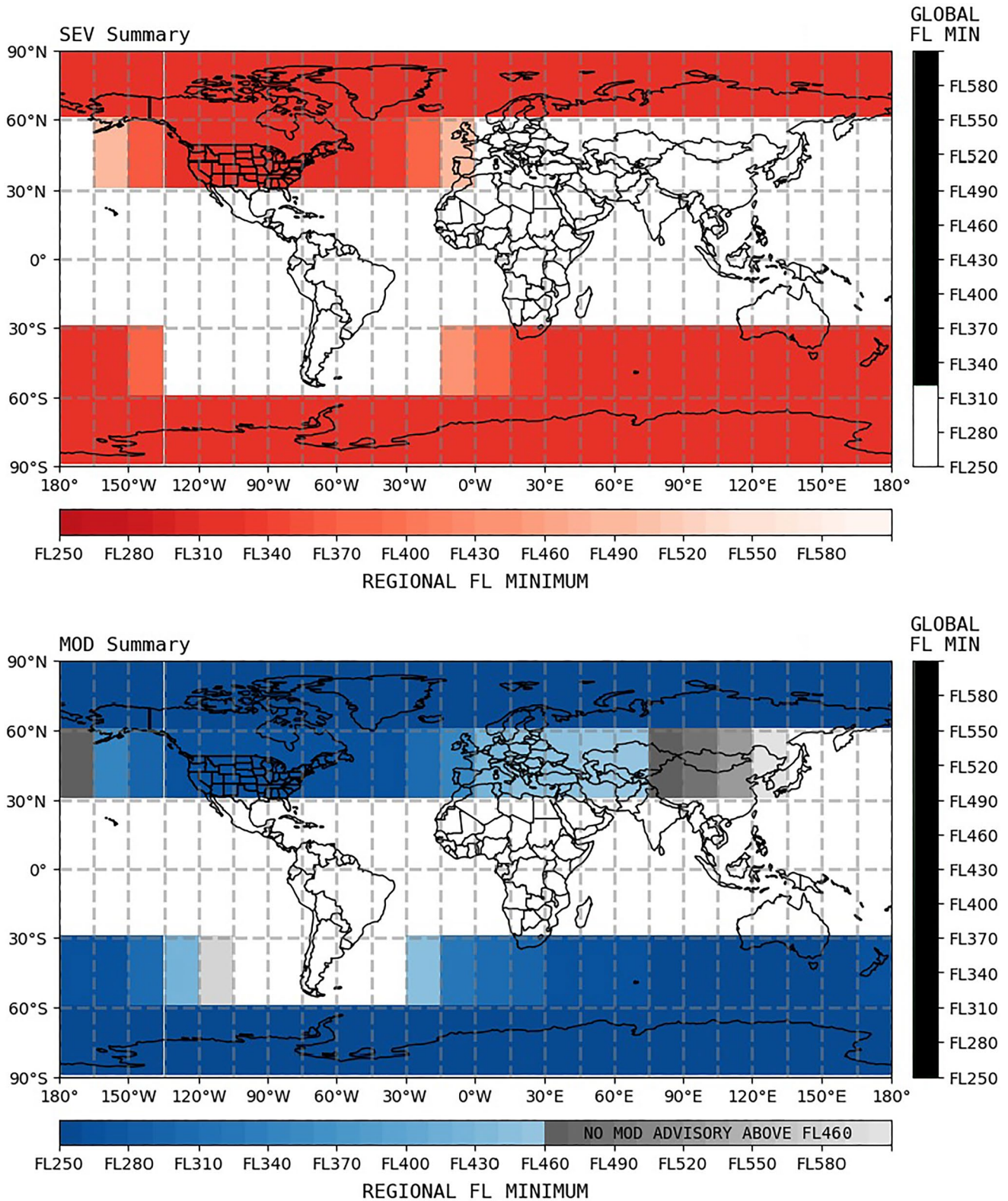


Figure 3. CARI-7A radiation summary maps thresholded to show regions exceeding the SEV (top:red) and MOD (bottom:blue/gray) ICAO thresholds. Shaded gray cells in the MOD summary map (bottom) show regions \leq FL460 where the radiation effective dose rate has surpassed the MOD threshold, but for which an advisory is not required. Horizontal regional FL Minimum colorbar indicates the minimum flight level reached in each individual region. The vertical global FL minimum colorbar shows the lowest flight level reached globally. The inclusion of MOD and SEV advisories at mid geographic latitudes, due to the tilt of the geomagnetic pole, is discussed Section 6.

Table 4
ICAO Radiation Advisories for GLE69 on the 20th of January 2005

Issue time (UT)	Advisory	Latitude	Longitude	Flight levels
2005-01-20 06:55	SEV	HNH MNH MSH HSH	E180–W180	ABV FL320
2005-01-20 06:55	MOD	HNH MNH MSH HSH	E180–W180	ABV FL250
2005-01-20 07:25	SEV	HNH MNH MSH HSH	E180–W180	ABV FL410
2005-01-20 07:25	MOD	HNH MNH MSH HSH	E180–W180	ABV FL320
2005-01-20 08:00	SEV	HNH MNH MSH HSH	E180–W180	ABV FL470
2005-01-20 08:25	MOD	HNH MNH MSH HSH	E180–W180	ABV FL390
2005-01-20 10:15	SEV	HNH MNH MSH HSH	E180–W180	ABV FL540
2005-01-20 11:05	MOD	NO SWX EXP		
2005-01-20 12:20	SEV	HNH MNH MSH HSH	E180–W180	ABV FL600
2005-01-20 13:30	SEV	NO SWX EXP		

the mid latitude range, based on model guidance and the impacts to users. A shift to advisories composed of polygon-based regions with finer spatial resolution, rather than entire geographic latitude bands, is critical and is being considered for future updates to the ICAO advisory format.

5.3.2. Timeline for GLE69 Radiation Impacts

A timeline of ICAO advisories for GLE69 is shown in Table 4. At the event onset a SEV advisory would have taken priority and been issued first, for the threshold crossing which occurred at 06:55 UTC, for four latitude bands (HNH, MNH, MSH, and HSH) above FL320. In practice, due to latency in receiving the GOES proton (1–2 min) and neutron monitor data (~5–10 min) used as inputs to the model, and model run time with post processing (3–4 min), as well as forecaster review and issue time (5–10 min), ICAO advisories may realistically be issued with a latency of 20–25 min with respect to changes in the environment. With a lower priority (in respect to the SEV advisory), a MOD advisory for the same four latitude bands above FL250 would have followed a few minutes after the SEV advisory, taking into account the time for a forecaster to compile and issue this second advisory. For simplicity, the modeling results presented here ignore data and modeling latencies, as well as the variable human-in-the-loop reaction time, in order to highlight the ICAO advisory progression as pertains to the changes to the physical radiation environment and issuing best practices. Included in the issue times are the suggested requirements of waiting at least 30 min between advisories, and observing three consecutive 5 minute intervals which show a change in altitude of at least 6,000 ft.

Figure 4 shows the evolution of impacted flight levels throughout the event for the polar (HNH and HSH) and mid latitude (MNH and MSH) bands. Vertical lines indicate the timing of SEV (solid) and MOD (dashed) advisory updates. After the rapid onset and peak, the effective dose rates decreased quickly at first, then more gradually over the next 6 hr, and subsequently fewer flight levels were impacted. Based on CARI-7A modeling, 10 advisories would have been issued (including two termination messages) and in effect for about six and a half hours. From 10:20 UTC the MOD threshold is no longer exceeded at or below FL460, and a termination would have been issued 45 min later at 11:05 UTC. The advisory remarks would note that a SEV advisory is still in place. At 12:45 UTC the SEV threshold is no longer exceeded, and a termination for the SEV advisory would have been issued at 13:30 UTC.

6. Discussion

The period from January 15th to 20th 2005 provides a fortuitous demonstration of the range of SWPC's proton and solar radiation storm products and services. Over the course of a week, the series of SEP events observed at Earth became gradually more impactful, growing in energy and intensity with each event. From the retrospective modeling of GLE69, and feedback from the Experiment, there are several key takeaways:

1. *S3 proton Alerts versus ICAO radiation advisories.* A comparison of the events on the 17th and 20th of January highlights the importance of atmospheric radiation advisories for users in the aviation industry. Where

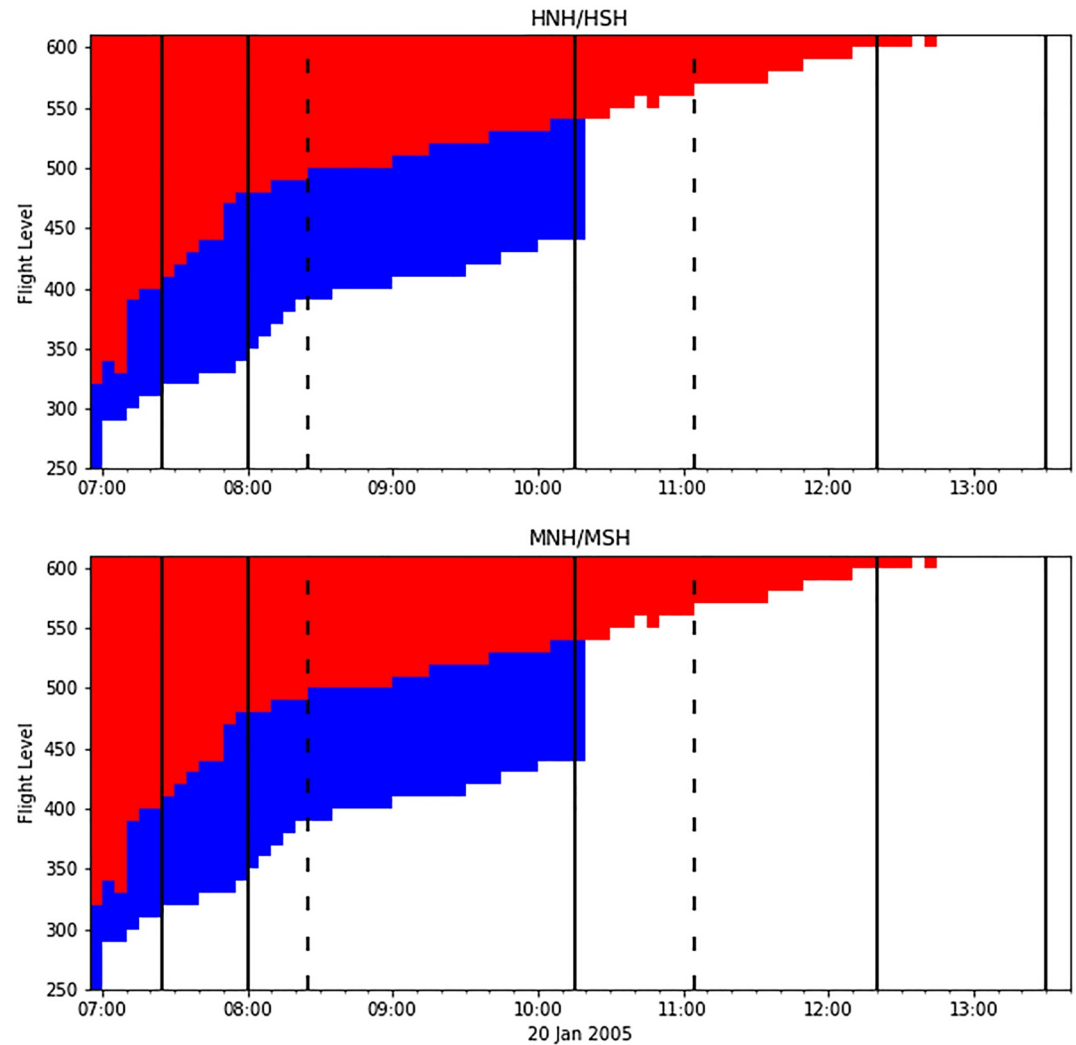


Figure 4. Evolution of the flight levels which exceed SEV (red) and MOD (blue) thresholds, for the HNH/HSH (top) and MNH/MSH (bottom) latitude bands during GLE69. Black vertical lines indicate times when the SEV (solid) and MOD (dashed) advisories would be updated based on a 6,000 ft flight level change.

the aviation industry has in the past used the S3 level to guide its response to a potential SEP-related radiation health hazard, these two S3 events, one with and one without ICAO advisories, showcase how the information contained in the ICAO advisories could be used by operators to better inform their practices. Without a significant enhancement to the radiation environment at aviation altitudes on the 17th, there was no reason to reroute or delay flights in the polar region from a health perspective, saving time and money (note: impacts to HF communications from PCA may still have disrupted flights in these regions). There is also precedence for smaller S2 proton events to result in a GLE and exceed the SEV threshold within the ICAO flight level range (e.g., the 13th of December 2006 S2 proton event which resulted in GLE70, the details of which are beyond the scope of this paper) further highlighting the inadequacies of the ≥ 10 MeV based S-scale for informing the decisions made by users in the aviation industry.

2. *ICAO advisory spatial requirements.* ICAO radiation advisories are currently based on complete geographic latitude bands only. This leads to several problems:

- (a) As the atmospheric radiation environment is dictated by the geomagnetic field and associated particle access, the severity of radiation exposure is centered around the geomagnetic poles. This leads to an offset between the geomagnetic coordinate system defined by the environment and the geographic grid required by ICAO. As seen in the example above, this offset makes it difficult to issue an advisory in the

- format currently required by ICAO without it including regions which do not exceed the threshold. This will lead to large areas being issued an advisory unnecessarily and cause confusion for aviation operators.
- (b) The defined latitude bands are wide. Should any portion of the latitude band exceed the MOD or SEV thresholds, the full latitude band will be included in the advisory. In the northern hemisphere this will result in relatively low latitude U.S. domestic flights receiving an unnecessary advisory if for example, southern Canada should exceed a threshold.
 - (c) The current agreement to mirror advisories in the northern and southern hemispheres may lead to an exaggeration of the radiation dose rate severity for some regions during the onset and peak of some SEP events, which can exhibit large anisotropies in the particle flux (Bütikofer et al., 2008). Although not modeled here, the January 20th event showed a large anisotropy at the event onset, with neutron monitor stations in Antarctica showing 1968% (South Pole) and 2389% (Terre Adiele) increases above background versus high latitude stations in the northern hemisphere showing around 150%–250%. Such anisotropies can lead to significantly different dose rates in regions of the globe with similar geomagnetic shielding and ICAO advisories should reflect this variation. Model development is required for CARI-7A to handle anisotropies in operations.

The ICAO advisories should be revised to include the use of polygons, ideally oriented on a geomagnetic grid, with appropriate spatial resolution and no requirement for the advisories to be mirrored across hemispheres.

3. *Timing of advisory updates and termination.* As noted before, radiation advisories should be updated every 6 hr or earlier given a significant change to the radiation environment that is, a change to the threshold level or a change in the impacted area, either geographically or to the impacted flight levels by at least 6,000 ft. The results above follow the suggested best practice of waiting 30 min before updating an advisory and at least 45 min before terminating an advisory. However, further feedback from users is required to determine whether this is appropriate for the aviation industry. For the advisories to be effective they should communicate improving or worsening conditions. As is seen in GLE69, conditions can change rapidly during the peak and immediate decay of the event, resulting in a number of advisories being issued in quick succession. The frequencies of updates should balance a concern for overalerting customers with a bombardment of notifications versus updating them promptly when conditions improve or worsen. GLE69 represents a particularly energetic and prompt SEP event, the largest of the solar cycle. Over this period 10 advisories would have been issued over ~6.5 hr, with the shortest wait between advisories being 30 min by design. During such an extreme event, the frequent advisories are warranted, but feedback from aviation operators should be taken into account and folded into standard operating procedures for forecasters. This feedback could allow forecasters to appropriately update and terminate advisories at their discretion while balancing agreed upon best practices.
4. *Flight Level resolution.* ICAO advisories can be specified with 1,000 ft vertical resolution. However, there have not been enough radiation measurements made during SEP events to validate models and confirm that such fine vertical resolution can be accurately achieved by current models. Initial comparisons between the models run in operations by different ICAO centers reveal inconsistencies in MOD and SEV Flight Level boundaries of up to ~10,000 ft. The results of these comparisons will be published in a future manuscript and should be used to appropriately set the vertical flight level requirements for ICAO advisories.
5. *Nowcasts versus Forecasts.* Currently, SWPC ICAO radiation advisories are issued as nowcasts only, with users noting that this provides limited actionable information. Accurate, real-time forecasts of SEP particle intensities and spectra, and the geomagnetic field, are required to provide users with information about the duration and severity of an event prior to and during an event.

Adoption of the new ICAO radiation advisories will require the revision of standard operating procedures used by operators. However, significant work remains to make the advisories actionable and ensure an appropriate response by pilots and air traffic planners/controllers. Continued user engagement, including education and training, is required.

Finding appropriate solutions to these problems requires not just input from users, but also consideration of the known model capabilities and uncertainties (Bain et al., 2023). For example, uncertainties in the characterization of the Earth's magnetic field, particularly during periods of dynamic solar wind and during the passage of interplanetary CMEs when the geomagnetic field is disturbed, can lead to dose rate uncertainties. At such times, the boundary between open and closed field can shift several degrees toward the equator, exposing lower latitudes to higher radiation dose rates (Kress et al., 2010; Mertens et al., 2010). This is particularly significant for flight

routes between the for example, continental U.S. and Europe, which fly parallel and close to the open/closed boundary, and for determining whether these flights are being exposed to elevated radiation dose rates or not. Uncertainty in the determination of the geomagnetic field in these regions can result in dose rate uncertainties ranging from a factor of two to an order of magnitude or more, depending on the level of geomagnetic storming (Mertens et al., 2010). ICAO radiation advisories should adopt an appropriate spatial resolution which takes into account the degree to which the geomagnetic field can be accurately represented.

Observations which characterize the atmospheric radiation environment are required to validate and improve models. While there have been several measurement campaigns (Benton, 2004; Gersey et al., 2012; Goldhagen et al., 2002; Mertens et al., 2016; Tobiska et al., 2018), with a few exceptions (Beck et al., 2008; Dyer et al., 2003), these campaigns were carried out in the absence of an SEP event, when the GCR background was the dominant source of ionizing radiation. Generally speaking, these studies found the modeled GCR-induced radiation environment to be in good agreement with observations (Bottollier-Depois et al., 2009). However further campaigns are required to validate models during large SEP events, particularly as there can be large uncertainties associated with the characterization of the primary SEP proton spectra used as an input to the model and therefore in the resulting SEP-induced dose rates. Systematic measurements of linear energy transfer spectra (LET) spectra and total ionizing dose are crucial for validating models and obtaining a better understanding of the spatial and temporal features of the atmospheric radiation environment (Dyer et al., 2018; Hayes et al., 2022; Lee et al., 2023; Meier et al., 2016; Mertens et al., 2016; Tobiska et al., 2016).

In light of model uncertainties associated with current radiation environment modeling, efforts are underway to quantify uncertainties between the models run by the different ICAO space weather centers to determine the level of consistency that might be expected between these centers.

7. Summary

In this paper we presented observations and retrospective modeling for a series of SEP events which occurred in January 2005, to demonstrate SWPC's current suite of solar proton Warning and Alert products and new ICAO radiation advisories. We include a summary of the FAA CARI-7A aviation radiation model used to retrospectively model GLE69 and the model outputs that are used at SWPC in real time operations. We demonstrate that proton forecasts based on the S-scale for low energy, ≥ 10 MeV protons in geostationary orbit do not directly communicate to users whether there is a significant enhancement to the radiation environment in the atmosphere, as experienced by aviation flight crew and passengers. From two back to back S3 proton events we show how ICAO radiation advisories can provide that contextual information for aviation operators and complement SWPC's short term proton Warning and Alert products. However, we also identify places where the ICAO advisories should be improved.

During GLE69 we found that both ICAO SEV and MOD radiation thresholds would have been exceeded throughout the event onset, peak and decay. This particularly large SEP event would have resulted in a SEV advisory at the event onset, for the polar and mid latitudes in both north and south hemispheres, down to FL320. A MOD advisory would also have been issued for these regions further covering altitudes down to FL250. Over the course of 6.5 hr the effective dose rate decreased, impacting fewer flight levels. Following ICAO requirements and the best practice to update advisories when the environment significantly improves or worsens (i.e., a change in threshold level, a change in geographic extent or a change in altitude of 6,000 ft or more), this would have resulted in the issuance of 10 advisories throughout the event, including two messages which terminated the SEV and MOD advisory chains once the effective dose rate dropped back below threshold. The shortest period between updates would have been 30 min, as defined by current agreed upon best practices.

While radiation exposure can be reduced by rerouting aircraft and/or reducing flight altitude, this can result in increased costs due to extended flight times and fuel consumption. Significant work remains to make the ICAO advisories accurate and actionable, to remove the potential for regions to receive unnecessary advisories, and ensure the appropriate response of pilots and air traffic planners/controllers to the issuance of ICAO radiation advisories. Learning outcomes from the 2022 Testbed Experiment will be used to further improve SWPC services for the aviation industry. This will require sustained engagement between forecast providers and operators, and include user education and training, as well as continued research and development to improve modeling capabilities.

Appendix A: CARI-7A Model Description

A1. GCR Model

The GCR spectrum is comprised predominantly of energetic protons (89%) and He-ions (14%), but also of highly ionized heavy ion species. These highly ionized particles are influenced by the magnetic field throughout the Heliosphere and interplanetary space. As such, the GCR flux varies slowly over time, in tune with the 11 years solar cycle (Herbst et al., 2010). At solar maximum the relatively more complex magnetic field present in the solar wind scatters low energy GCR particles, reducing the number of particles reaching Earth. The GCR flux recorded at Earth therefore varies inversely with the solar cycle, increasing by around a factor of two from solar maximum to solar minimum. The GCR periodicity is offset by several months from the solar cycle, reflecting the propagation time of the solar magnetic field out into the Heliosphere.

CARI-7A has four options for modeling the GCR spectrum. The version of CARI-7A running operationally at NOAA SWPC currently uses the International Standard Organization (ISO) GCR model (ISO, 2004). The ISO GCR model is based on a time invariant Local Interstellar Spectrum (LIS) originating outside the Heliosphere and consisting of electrons and ions, from protons to uranium, with energies ≥ 10 MeV/nuc. In CARI-7A, the LIS spectrum can be modulated using two approaches: the method described in the ISO standard, a solar modulation potential based on solar activity levels indexed by sunspot number; or by heliocentric potential characterized by secondary neutron flux recorded by neutron monitors. The former is used in SWPC operations. The incident GCR spectra, consisting of particle spectra for H-Ni ions from 10 MeV to 10 TeV, is used as an input to CARI-7A and updated once per month for solar modulation, using monthly mean sunspot numbers from the World Data Center SILSO, Royal Observatory of Belgium (SILSO World Data Center, 2005) to modulate the GCR flux. Options to use the Badhwar & O'Neill 2011 GCR model (BON11) (O'Neill, 2010; O'Neill & Foster, 2013) or the Badhwar & O'Neill 2014 GCR model (BON14) (O'Neill et al., 2015) are available but not currently used in forecast operations.

Forbush decreases, that is, decreases in the observed GCR flux caused by the scattering of GCR particles by the complex magnetic field configurations in propagating CMEs, are handled in the CARI-7A model by modulating the GCR flux in a 1:1 ratio with changes in a high-latitude, near-sea-level neutron monitor (e.g., Oulu) count rates relative to the monthly average (Copeland, 2014; Lantos, 2005)

$$\phi_t = \phi_{\text{month}} \frac{N_t}{N_{\text{month}}} \quad (\text{A1})$$

where ϕ_t and ϕ_{month} are the GCR flux at the time of the model run and the average over the past month respectively, and N_t and N_{month} are the corresponding Oulu neutron monitor count rates.

A2. SEP Spectral Extrapolation

For the case study presented here, the SEP spectral component is initially characterized using proton measurements from GOES 11 Energetic Particle Sensor and High Energy Proton and Alpha Detector instruments (Sauer, 1989), which were used in forecast operations during 2005. The global ground-based neutron monitor network is then used to scale the high energy portion of the SEP proton spectrum. Neutron monitors capture the response of the atmosphere to penetrating particles, and observations from monitors situated in different geomagnetic locations can be used to infer the spectral shape of the incident particle spectra. A variety of approaches exist to extrapolate SEP spectra using GOES and/or neutron monitor data, for example, Matthiä et al. (2018). We use the extrapolation technique detailed in Copeland et al. (2008).

In this approach, neutron count rates are used to correct the highest rigidity portion of the GOES SEP proton spectrum ($\gtrsim 1,200$ MV) for each 5 minute interval throughout the SEP. Note the corrections are carried out as a function of rigidity, before being converted back to energy space for input into CARI-7. The high rigidity portion of the proton spectrum is divided into n rigidity zones, corresponding to neutron monitors in n geomagnetic cutoff rigidity zones, spanning high to low geomagnetic latitudes. The number of zones and the cutoff rigidity of each zone are based on the availability and distribution of neutron monitor stations at the time of the event. Count rates from high latitude and polar stations are averaged and counted as a single station for zone 0. For GLE69, the KIEL station is used for zone 1 and LMKS is used for zone 2. (ROME, MXCO and ESOI were available for

zones 3–5: however, none of these stations showed an increase above background). For each SEP time interval, correction factors are found for each rigidity zone and applied to the SEP proton spectrum as follows.

1. Using CARI-7A, neutron count rates are simulated from the background GCR ($C_{GCR(j)}$, where $j = 0-n$) at each of the neutron monitor station locations. An average count rate from the month preceding the event is used.
2. For each 5 minute interval during the SEP:
 - (a) Neutron count rates are simulated at each station resulting from an initial uncorrected SEP proton spectrum derived from GOES ($C_{SEP(j)}$).
 - (b) The simulated percent increase ($\pi_{sim(j)}$) between the pre-event GCR neutron count rate and the neutron count rate during the SEP event is calculated.

$$\pi_{sim(j)} = 100 \frac{C_{SEP(j)}}{C_{GCR(j)}} \quad (A2)$$

- (c) The simulated percent increase is compared with that observed by each station ($\pi_{obs(j)}$).
- (d) Starting with the highest rigidity zone, a correction factor, $C_z(j)$, is calculated for each zone using Equations A3 and A4.

$$\pi_{C(j)} = 100 \sum_{k=j+1}^n \frac{C_z(k) C_{SEP(k)}}{C_{GCR(j)}} \quad (A3)$$

$$C_z(j) = \frac{\pi_{obs(j)} - \pi_{C(j)}}{\pi_{sim(j)}} \quad (A4)$$

A negative $C_z(j)$ is set to zero. For Equation A4, $\pi_{C(j)}$ is the percent increase at station j resulting from flux in higher rigidity zones. Therefore, $\pi_{C(j=n)} = 0$.

- (e) The rigidity zones of the initial uncorrected proton spectrum from GOES are then multiplied by the rigidity-dependent correction factors.
3. The neutron monitor corrected SEP proton spectra is added to the proton component of the GCR spectra and used as an input to CARI-7.

The end result is a primary SEP proton spectrum that reproduces the ground-based neutron monitor measurements. For a detailed methodology the reader should consult Copeland et al. (2008). This approach has the benefit of maintaining consistency between neutron monitor observations and the energy dependent particle flux required to generate those observations. This approach does not result in a smooth proton spectrum found with common single or double power law parametric forms. However, smooth parametric forms can impose spectral slopes when fitting the data which over or under estimate the particle flux at the high energies most important for the radiation dose rate at aviation altitudes. It should be noted that the current SWPC implementation of CARI-7A uses only GOES particle data to extrapolate the SEP proton spectra. A upgraded version of the spectral extrapolation which uses near real-time neutron monitor data will be implemented soon.

A3. Geomagnetic Response

The rigidity required for an energetic particle gaining access to the magnetosphere is a function of the particle's direction of incidence and location in the magnetosphere (Störmer, 1956). Different approaches have been developed to model global geomagnetic cutoffs, from simulations which trace particle trajectories (Kress et al., 2004, 2010; Mertens et al., 2010) to precalculated cutoff rigidity tables based on an empirical magnetic field model that is characterized by the geomagnetic index K_p (Smart et al., 2000; Smart & Shea, 2005).

The time constraints imposed by computationally intensive particle trajectory tracing codes are not currently convenient for implementation in an real-time operational setting, nor are the well used Smart and Shea (2005) cutoff rigidity tables, which are based on K_p (available in 3 hr increments). For SWPC ICAO advisories we have chosen an empirical relationship for R_c which is based on the Dst index, which has a 1 hour cadence, developed by Ogliore et al. (2001), updated by Leske et al. (2001) and described in O'Brien et al. (2018). We use this approach for modeling the geomagnetic field during GLE69.

$$R_c = 15.062 \cos^4(\Lambda_c + Dst/19.11) - 0.363 \quad (A5)$$

where Λ_c is the cutoff invariant latitude in degrees and Dst is in nanotesla. L shell values are obtained from the International Geomagnetic Reference Field model hosted by the Community Coordinated Modeling Center. Values for Dst are obtained from the Kyoto archive. Λ_c is then determined from L.

$$\cos \Lambda_c = \frac{1}{\sqrt{L_c}} \quad (\text{A6})$$

Values for R_c are determined for a global $1^\circ \times 1^\circ$ spatial grid and pre-calculated and stored for a wide range of Dst values. As the Dst index is updated once an hour the appropriate lookup table is selected for use.

A4. Atmospheric Response

Both GCR and SEP particles interact with Earth's atmosphere in the same manner, but with a different mix of incident particle flux and energy distributions. The atmosphere is an effective shield near sea level, equivalent to approximately 10 m of water, but this lessens rapidly as altitude increases. The model atmosphere used in CARI-7A is based on the 1976 U.S. Standard Atmosphere (NOAA, 1976), but differs from that standard in that the total distance from the vacuum of outer space (0 kg m^{-3}) to sea level is fixed at 100 km (328,000 ft.) and is divided into 1 km deep spherical shells of constant density. Below the lowest atmospheric shell, the Earth is modeled as a sphere of liquid water of radius 6371 km and density 10^3 kg m^{-3} (1 g cm^{-3}) from which particles are allowed to enter (or return) to the atmosphere. Particles leaving the atmosphere to enter space (upward moving particles that leave the model space) are deemed lost. The model atmosphere has a total vertical column depth of 1035.1 g cm^{-2} and for calculating dose rate, instrument responses, etc., particle flux data are ordered and interpolated using atmospheric depth. The atmospheric response to cosmic ray entry is derived from a database of pre-calculated Monte Carlo simulations (MCNPX 2.7.0 Oak Ridge National Laboratory (2011)) of cosmic ray showers. The primary particle entries simulated using MCNPX were of H-Fe atomic nuclei and neutrons. Primary energies in simulations ranged from 10 MeV to 1 TeV and used a 1, 2, 5...decadal grid. For all showers, particles tracked in MCNPX were kaons, pions, muons, photons, electrons, neutrinos, neutrons, protons, deuterons, tritons, alphas, and other atomic nuclei up to iron. For more details on atmospheric response modeling in CARI-7A see Copeland (2017) and Copeland (2021).

A5. Model Outputs

For real-time operations, when timely results are required, CARI-7A is used to calculate the effective dose rates at 17 integer value cutoff rigidities between 0 and 17 GV. Then interpolation of the effective dose rate as a function of rigidity is used to gain finer detail. Using the pre-calculated rigidity lookup table from Appendix A3, effective dose rates are mapped to locations on the global map, to create radiation dose rate maps as a function of altitude, such as the example in Figure 1.

Data Availability Statement

GOES proton data used as an input to CARI-7 is archived at NOAA NCEI <https://www.ncei.noaa.gov/data/goes-space-environment-monitor/access/avg/>. The Dst data used in this paper was provided by the World Data Center for Geomagnetism, Kyoto (<http://wdc.kugi.kyoto-u.ac.jp/wdc/Sec3.html>, Nose et al. (2015)). Sunspot number data is available from the World Data Center Sunspot Index and Long-term Solar Observations (SILSO), Royal Observatory of Belgium (SILSO World Data Center, 2005). Neutron monitor data is accessible via the NMDB database <https://www.nmdb.eu>, founded under the European Union's FP7 program (contract no. 213007), from the following institutes: the neutron monitor data for the Apatity neutron monitor is provided by the Polar Geophysical Institute Russian Academy of Sciences; the neutron monitor data from Fort Smith, Inuvik, Nain, Peawanuck and Thule stations are provided by the University of Delaware Department of Physics and Astronomy and the Bartol Research Institute; the neutron monitor data from Oulu are provided by the Sodankyla Geophysical Observatory; the neutron monitor data from Kiel are provided by the Extraterrestrial Physics Department of the Institute for Experimental and Applied Physics of the Christian-Albrechts University of Kiel and the operation of the Lomnický štít neutron monitors is supported by Slovak grant agency APVV (project no. 51-053805). The Monte Carlo N-Particle physics simulation program (MCNPX 2.7.0) and associated particle cross section databases used to generate the pre-calculated showers that form the basis of fluence to dose conversion in

CARI-7A are available from <https://www-rsicc.ornl.gov/codes/ccc/ccc7/ccc-740.html> (Oak Ridge National Laboratory, 2011). The processed particles shower files that are the basis of CARI-7A are available with the downloaded copy of CARI-7A (https://www.faa.gov/data_research/research/med_humanfacs/aeromedical/radiobiology/cari7, (Copeland, 2021)).

Acknowledgments

Author HMB carried out this work while supported by NOAA cooperative agreements NA17OAR4320101 and NA22OAR4320151.

References

- Abt Associates, I. (2019). Customer needs and requirements for space weather products and services. [Computer software manual]. National Oceanic and Atmospheric Administration. <https://repository.library.noaa.gov/view/noaa/29107>
- Annex 3 to the convention on international civil aviation, meteorological service for international air navigation, ICAO international standards and recommended practices (SARPS). (2018). Annex 3 to the convention on international civil aviation, meteorological service for international air navigation, ICAO international standards and recommended practices (SARPS). [Computer software manual]. ICAO. Retrieved from <https://store.icao.int/en/annex-3-meteorological-service-for-international-air-navigation>
- Bain, H. M., Onsager, T. G., Mertens, C. J., Copeland, K., Benton, E. R., Clem, J., et al. (2023). Improved space weather observations and modeling for aviation radiation. *Frontiers in Astronomy and Space Sciences*, *10*, 1149014. <https://doi.org/10.3389/fspas.2023.1149014>
- Bain, H. M., Steenburgh, R. A., Onsager, T. G., & Stitely, E. M. (2021). A summary of National Oceanic and Atmospheric Administration space weather prediction center proton event forecast performance and skill. *Space Weather*, *19*(7), e2020SW002670. <https://doi.org/10.1029/2020SW002670>
- Beck, P., Bartlett, D. T., Bilski, P., Dyer, C., Flückiger, E., Fuller, N., et al. (2008). Validation of modelling the radiation exposure due to solar particle events at aircraft altitudes. *Radiation Protection Dosimetry*, *131*(1), 51–58. <https://doi.org/10.1093/rpd/ncn238>
- Benton, E. (2004). Radiation dosimetry at aviation altitudes and in low-Earth Orbit. Ph.D. thesis. University College Dublin, Department of Experimental Physics.
- Bottollier-Depois, J. F., Beck, P., Bennett, B., Bennett, L., Bütikofer, R., Clairand, I., et al. (2009). Comparison of codes assessing galactic cosmic radiation exposure of aircraft crew. *Radiation Protection Dosimetry*, *136*(4), 317–323. <https://doi.org/10.1093/rpd/ncp159>
- Bütikofer, R., Flückiger, E., Desorgher, L., & Moser, M. (2008). The extreme solar cosmic ray particle event on 20 January 2005 and its influence on the radiation dose rate at aircraft altitude. *Science of the Total Environment*, *391*(2), 177–183. <https://doi.org/10.1016/j.scitotenv.2007.10.021>
- Copeland, K. A. (2014). *Cosmic ray particle fluences in the atmosphere resulting from primary cosmic ray heavy ions and their resulting effects on dose rates to aircraft occupants as calculated with MCNPX 2.7.0*. A doctoral thesis at the Royal Military College of Canada (RMCC).
- Copeland, K., Sauer, H. H., Duke, F. E., & Friedberg, W. (2008). Cosmic radiation exposure of aircraft occupants on simulated high-latitude flights during solar proton events from 1 January 1986 through 1 January 2008. *Advances in Space Research*, *42*(6), 1008–1029. <https://doi.org/10.1016/j.asr.2008.03.001>
- Copeland, K. A. (2017). CARI-7A: Development and validation. *Radiation Protection Dosimetry*, *175*(4), 419–431. <https://doi.org/10.1093/rpd/new369>
- Copeland, K. A. (2021). *CARI-7 documentation: Radiation transport in the atmosphere*. Federal Aviation Administration Office of Aerospace Medicine Report DOT/FAA/AM-21/5. Retrieved from https://www.faa.gov/sites/faa.gov/files/data_research/research/med_humanfacs/aeromedical/202105.pdf
- Cucinotta, F. A. (2015). Review of NASA approach to space radiation risk assessments for Mars exploration. *Health Physics*, *108*(2), 131–142. <https://doi.org/10.1097/hp.0000000000000255>
- Cucinotta, F. A., Hu, S., Schwadron, N. A., Kozarev, K., Townsend, L. W., & Kim, M.-H. Y. (2010). Space radiation risk limits and earth-moon-Mars environmental models. *Space Weather*, *8*(12). <https://doi.org/10.1029/2010SW000572>
- Cucinotta, F. A., Kim, M. Y., & Chappell, L. J. (2013). Space radiation cancer risk projections and uncertainties. In *NASA technical paper*. NASA TP-2013-217375.
- Dyer, A. C. R., Ryden, K. A., Hands, A. D. P., Dyer, C., Burnett, C., & Gibbs, M. (2018). Zenith: A radiosonde detector for rapid-response ionizing atmospheric radiation measurements during solar particle events. *Space Weather*, *16*(3), 261–272. <https://doi.org/10.1002/2017SW001692>
- Dyer, C., Lei, F., Clucas, S., Smart, D., & Shea, M. (2003). Calculations and observations of solar particle enhancements to the radiation environment at aircraft altitudes. *Advances in Space Research*, *32*(1), 81–93. [https://doi.org/10.1016/S0273-1177\(03\)90374-7](https://doi.org/10.1016/S0273-1177(03)90374-7)
- Gersey, B., Wilkins, R., Atwell, W., Tobiska, W. K., & Mertens, C. (2012). Tissue equivalent proportional counter microdosimetry measurements aboard high-altitude and commercial aircraft. In *42nd international conference on environmental systems*. AIAA 2012-3636.
- Goldhagen, P., Reginatto, M., Kniss, T., Wilson, J. W., Singleterry, R. C., Jones, I. W., & Van Steveninck, W. V. (2002). Measurement of the energy spectrum of cosmic-ray induced neutrons aboard an ER-2 high-altitude airplane. *Nuclear Instruments and Methods*, *476*(1–2), 42–51. [https://doi.org/10.1016/S0168-9002\(01\)01386-9](https://doi.org/10.1016/S0168-9002(01)01386-9)
- Hayes, B. M., Causey, O. I., Gersey, B. B., & Benton, E. R. (2022). Active tissue equivalent dosimeter: A tissue equivalent proportional counter flown onboard the international space station. *Nuclear Instruments and Methods in Physics Research Section A: Accelerators, Spectrometers, Detectors and Associated Equipment*, *1028*, 166389. <https://doi.org/10.1016/j.nima.2022.166389>
- Herbst, K., Kopp, A., Heber, B., Steinhilber, F., Fichtner, H., Scherer, K., & Matthiä, D. (2010). On the importance of the local interstellar spectrum for the solar modulation parameter. *Journal of Geophysical Research*, *115*(D1), D00120. <https://doi.org/10.1029/2009JD012557>
- ISO, I. S. O. (2004). *Space environment (natural and artificial)—galactic cosmic ray model*, Tech. Rep. ISO 15390. American National Standards Institute. Retrieved from <https://www.iso.org/standard/76594.html>
- Koons, H. C., Mazur, J. E., Selesnick, R. S., Blake, J. B., Fennell, J. F., Roeder, J. L., & Anderson, P. C. (1999). The impact of the space environment on space systems. In *Aerospace tech. Rep., TR-99 (1670)-1*.
- Kress, B. T., Hudson, M. K., Perry, K. L., & Slocum, P. L. (2004). Dynamic modeling of geomagnetic cutoff for the 23–24 November 2001 solar energetic particle event. *Geophysical Research Letters*, *31*(4), L04808. <https://doi.org/10.1029/2003GL018599>
- Kress, B. T., Mertens, C. J., & Wiltberger, M. (2010). Solar energetic particle cutoff variations during the 29–31 October 2003 geomagnetic storm. *Space Weather*, *8*(5). <https://doi.org/10.1029/2009SW000488>
- Kress, B. T., Rodriguez, J. V., & Onsager, T. G. (2020). Chapter 20—The goes-r space environment in situ suite (seiss): Measurement of energetic particles in geospace. In S. J. Goodman, T. J. Schmit, J. Daniels, & R. J. Redmon (Eds.), *The goes-r series* (pp. 243–250). Elsevier. <https://doi.org/10.1016/B978-0-12-814327-8.00020-2>
- Lantos, P. (2005). Forbush decrease effects on radiation dose received on-board aeroplanes. *Radiation Protection Dosimetry*, *117*(4), 357–364. <https://doi.org/10.1093/rpd/nci302>

- Lee, T., & Benton, E. R. (2023). Dosimetric Measurements Aboard the NASA WB-57 High Altitude Research Aircraft: Preliminary Results. Zenodo. <https://doi.org/10.5281/zenodo.7662290>
- Leske, R. A., Mewaldt, R. A., Stone, E. C., & von Rosenvinge, T. T. (2001). Observations of geomagnetic cutoff variations during solar energetic particle events and implications for the radiation environment at the space station. *Journal of Geophysical Research*, *106*(A12), 30011–30022. <https://doi.org/10.1029/2000JA000212>
- Manual on space weather information in support of international air navigation (doc 10100). (2019). Manual on space weather information in support of international air navigation (doc 10100). [Computer software manual]. ICAO. Retrieved from <https://store.icao.int/en/manual-on-space-weather-information-in-support-of-international-air-navigation-doc-10100>
- Matthiä, D., Meier, M. M., & Berger, T. (2018). The solar particle event on 10–13 September 2017: Spectral reconstruction and calculation of the radiation exposure in aviation and space. *Space Weather*, *16*(8), 977–986. <https://doi.org/10.1029/2018SW001921>
- Meier, M. M., & Matthiä, D. (2014). A space weather index for the radiation field at aviation altitudes. *Journal of Space Weather and Space Climate*, *4*, A13. <https://doi.org/10.1051/swsc/2014010>
- Meier, M. M., Matthiä, D., Forkert, T., Wirtz, M., Scheibinger, M., Hübel, R., & Mertens, C. J. (2016). Rad-x: Complementary measurements of dose rates at aviation altitudes. *Space Weather*, *14*(9), 689–694. <https://doi.org/10.1002/2016SW001418>
- Mertens, C. J., Gronoff, G. P., Norman, R. B., Hayes, B. M., Lusby, T. C., Straume, T., et al. (2016). Cosmic radiation dose measurements from the RaD-X flight campaign. *Space Weather*, *14*(10), 874–898. <https://doi.org/10.1002/2016SW001407>
- Mertens, C. J., Kress, B. T., Wiltberger, M., Blattinig, S. R., Slaba, T. S., Solomon, S. C., & Engel, M. (2010). Geomagnetic influence on aircraft radiation exposure during a solar energetic particle event in October 2003. *Space Weather*, *8*(3). <https://doi.org/10.1029/2009SW000487>
- Mertens, C. J., & Slaba, T. C. (2019). Characterization of solar energetic particle radiation dose to astronaut crew on deep-space exploration missions. *Space Weather*, *17*(12), 1650–1658. <https://doi.org/10.1029/2019SW002363>
- Nose, M., Iyemori, T., Sugiura, M., & Kamei, T. (2015). World data center for geomagnetism. [Dataset]. Kyoto. <https://doi.org/10.17593/14515-74000>
- Oak Ridge National Laboratory. (2011). Monte Carlo n-particle transport code system for multiparticle and high energy applications (MCNPX 2.7.0), RSICC code package C740. [Software]. Los Alamos National Laboratory. Retrieved from https://mcnp.lanl.gov/pdf_files/TechReport_2011_LANL_LA-UR-11-02295_PelowitzDurkeeEtAl.pdf
- O'Brien, T. P., Mazur, J. E., & Looper, M. D. (2018). Solar energetic proton access to the magnetosphere during the 10–14 September 2017 particle event. *Space Weather*, *16*(12), 2022–2037. <https://doi.org/10.1029/2018SW001960>
- Ogliore, R. C., Mewaldt, R. A., Leske, R. A., Stone, E. C., & von Rosenvinge, T. T. (2001). A direct measurement of the geomagnetic cutoff for cosmic rays at space station latitudes. In *International cosmic ray conference* (Vol. 10, p. 4112).
- O'Neill, P. M. (2010). Badhwar–O'Neill 2010 galactic cosmic ray flux model—Revised. *IEEE Transactions on Nuclear Science*, *57*(6), 3148–3153. <https://doi.org/10.1109/TNS.2010.2083688>
- O'Neill, P. M., & Foster, C. C. (2013). Badhwar–O'Neill 2011 galactic cosmic ray flux model description. Tech. Rep. NASA/TP-2013-217376.
- O'Neill, P. M., Gogle, S., & Slaba, T. C. (2015). Badhwar–O'Neill 2014 galactic cosmic ray flux model description. Tech. Rep. NASA/TP-2015-218569.
- Rodriguez, J. V., Krosschell, J. C., & Green, J. C. (2014). Intercalibration of GOES 8–15 solar proton detectors. *Space Weather*, *12*(1), 92–109. <https://doi.org/10.1002/2013SW000996>
- Sauer, H. H. (1989). SEL monitoring of the earth's energetic particle radiation environment. In *High-Energy Radiation Background in Space* (Vol. 186, pp. 216–221). <https://doi.org/10.1063/1.38171>
- SILSO World Data Center. (2005). The international sunspot number [Dataset]. International Sunspot Number Monthly Bulletin and Online Catalogue. Retrieved from <http://www.sidc.be/silso/>
- Smart, D. F., & Shea, M. A. (2005). A review of geomagnetic cutoff rigidities for earth-orbiting spacecraft. *Advances in Space Research*, *36*(10), 2012–2020. <https://doi.org/10.1016/j.asr.2004.09.015>
- Smart, D. F., Shea, M. A., & Flückiger, E. O. (2000). Magnetospheric models and trajectory computations. *Space Science Reviews*, *93*(1), 305–333. <https://doi.org/10.1023/A:1026556831199>
- Störmer, C. (1956). The polar aurora. by Carl Störmer. Oxford University Press, 1955. pp. xvii, 403; 216 figs., 27 tables. 55s. *Quarterly Journal of the Royal Meteorological Society*, *82*(351). <https://doi.org/10.1002/qj.49708235123>
- Tobiska, W. K., Bouwer, D., Smart, D., Shea, M., Bailey, J., Didkovsky, L., et al. (2016). Global real-time dose measurements using the automated radiation measurements for aerospace safety (ARMAS) system. *Space Weather*, *14*(11), 1053–1080. <https://doi.org/10.1002/2016SW001419>
- Tobiska, W. K., Didkovsky, L., Judge, K., Weiman, S., Bouwer, D., Bailey, J., et al. (2018). Analytical representations for characterizing the global aviation radiation environment based on model and measurement databases. *Space Weather*, *16*(10), 1523–1538. <https://doi.org/10.1029/2018SW001843>